Single Cell Peptide Heterogeneity of Rat Islets of Langerhans

Erik T. Jansson†, Troy J. Comi, Stanislav S. Rubakhin, and Jonathan V. Sweedler*

Department of Chemistry and the Beckman Institute for Advanced Science and Technology, University of Illinois at Urbana–Champaign, Urbana, Illinois 61801, United States

Corresponding Author

* Phone: 217-244-7359. Email: jsweedle@illinois.edu.

Present Addresses

† Department of Chemistry, Stanford University, Stanford, California 94305, United States.

SUPPORTING INFORMATION

Additional Methods
Supporting Figures 1–6
Supporting Table 1

Additional Methods

Improved Precision and Throughput of Microscopy-guided Single Cell MALDI MS

To facilitate the accurate targeting of small (<10 µm) features located at distances of more than 1 cm, as well as to enable high throughput MALDI MS profiling, multiple enhancements have been made over our previous efforts. After samples were deposited on ITO glass slides, cell finding and registration were performed via a custom Python graphical user interface, automating many manual steps from the original protocol (see "Details of the Python Script for Cell Finding and Generating Custom XEO Geometry Files" section below, Figure S5, and Supplementary Software). The geometric transformation for generating mass spectral spatial coordinates developed in our laboratory was replaced with a probabilistic transformation using a point-based similarity algorithm. Point-based registration is more robust in preventing fiducial localization errors and decreases the target localization error by fourfold. When Gaussian noise, $N(\mu = 0$ µm, $\sigma = 100$ µm) was added to the fiducial coordinates, simulating fiducial localization uncertainty, the target localization error decreased from 164 ± 72 µm to 38 ± 15 µm (Figure S4), with the similarity transformation compared with the geometric transformation. Fluorescence images of cell suspensions deposited on ITO glass slides were acquired with a histological slide scanner, operating in batch mode with automatic image stitching. Finally, a custom MALDI matrix application system was designed to generate more consistent matrix coatings compared to manual artistic airbrush application (Figure S3); four slides can be coated simultaneously in less than 10 min.

MALDI MSI of regions surrounding individual cells suggests that analyte spreading is restricted to the first 50 µm, at which point the signal intensity drops to 10% of its peak value (Figure S4). The analyte spreading metric required a minimum 100 µm cell-to-cell distance to obtain single cell MALDI MS profiling data. Overall, we increased the robustness of the small cell localization process, and decreased the sample preparation time prior to MALDI MS acquisition from >2 h per sample to 45 min per sample.

Details of the Python Script for Cell Finding and Generating Custom XEO Geometry Files

The script and its dependent objects are provided as an additional Supporting information WinZip file (Supplementary Software.zip) containing blobFinder, mtpUtil, myNdpiSlide, and ndpiToXEOQT, along with a README file. The script should be operating system independent, though extensive testing was only performed on the Windows operating system. All .py files were written for Python 3.4 (www.python.org). The code requires the modules numpy, skimage, scipy, matplotlib, PyQt4, and openslide to be installed. The core modules are available in the SciPy package (www.scipy.org). Openslide may be obtained from http://openslide.org/.

The script initializes a graphical user interface (GUI) allowing the user to open .ndpi slide images. Any file type supported by openslide could be utilized, though the software was only extensively tested with .ndpi files. The user navigates around the image with mouse and keyboard controls. Hotkey information can be found under Help -> Hotkeys. Left clicking on a slide location moves that position to the center of the image and the scroll wheel zooms in and out of multilevel images. Pressing 't' switches between viewing brightfield and fluorescence images. To utilize this feature, ensure that the images are properly aligned and name the brightfield image with "bright", the fluorescence with "fluor".

Next, several fiducial markers should be selected to align the microscopy image with the Bruker mass spectrometer stage position. Fiducial locations are marked by right clicking at the center of the location to pop up an entry box. Shift + right click will remove the closest fiducial mark to the mouse location. Fiducials generated at predetermined MTP slide II adapter locations may be entered as the coordinate, e.g., "C5" (without quotes). Arbitrary stage locations may also be entered, for example as "-85475 -14235" for an x,y stage location of -85475, -14235 µm. Fiducial marks are displayed as blue circles

labeled with the closest grid location. Pressing ‘p’ will toggle predicted grid locations of the MTP slide II adapter as yellow circles.

Cell locations can be manually selected for interrogation by shift + left clicking on the object. Marked locations are displayed as a green circle. Manually placed locations may be removed by shift + left clicking within the green circle. Automatic cell finding requires careful selection of the cell finding parameters, found in Tools -> Blob Options. Selecting 'apply' will perform cell finding on the current image location at the maximum zoom level. Switching to threshold view (Ctrl + B) can assist with determining why some cells are selected while others are rejected. With the correct parameters, cell finding can be performed on the entire slide (default) or within a rectangular region of interest by drawing a yellow rectangle with Ctrl + left click and drag. During cell finding, the progress will be reported to console; the GUI will appear to freeze. Once completed, a base file name is requested for saving the information from that cell finding procedure. The registration information (_reg.txt), cell finding parameters with locations and sizes (_find.txt), and an xeo file are all saved (no suffix), and then the cell locations are drawn to screen. This step can be time consuming but all data is saved prior to drawing the found cell locations. The produced XEO file may be utilized for AutoXecute profiling with Bruker fleXanalysis software.

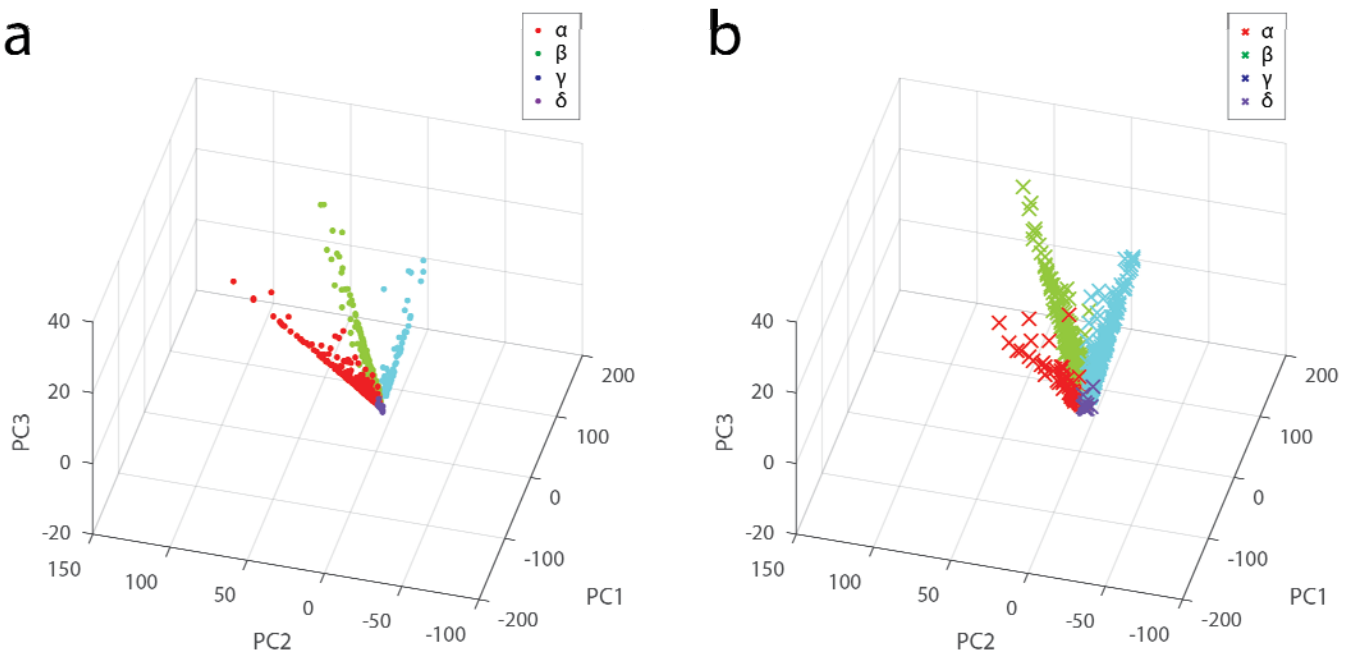

Figure S1. PCA allows visualization of the four canonical cell types observed with MALDI MS using principal components 1–3.

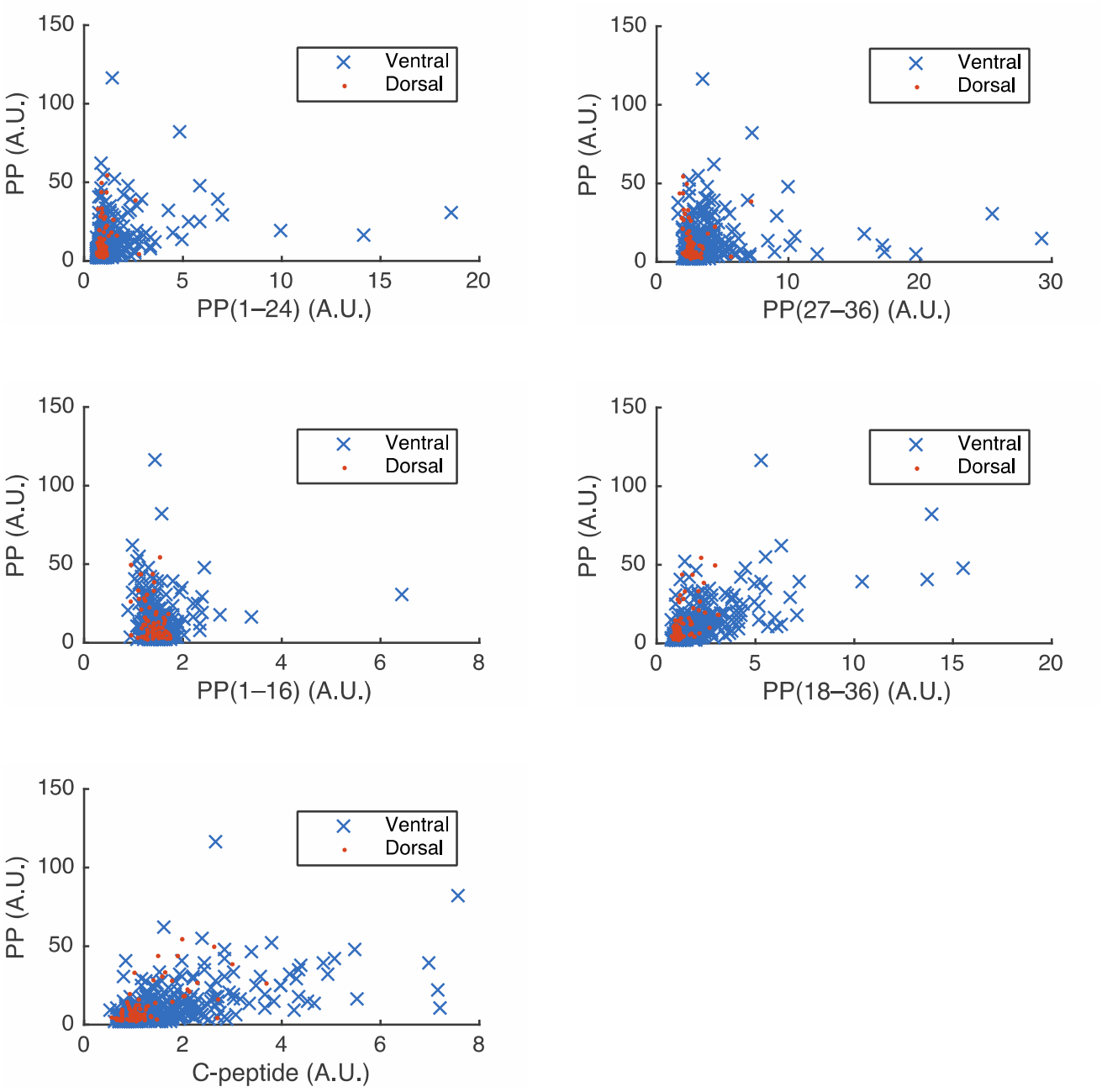

Figure S2. MALDI MS signal intensity of PP plotted against the signal intensities of PP(1–24), PP(27–36), PP(1–16), PP(18–36), and the C-terminal peptide from the pancreatic prohormone within single γ-cells ($n_{D\gamma}$ = 79 cells, $n_{V\gamma}$ = 418 cells) from ventral and dorsal islets are compared.

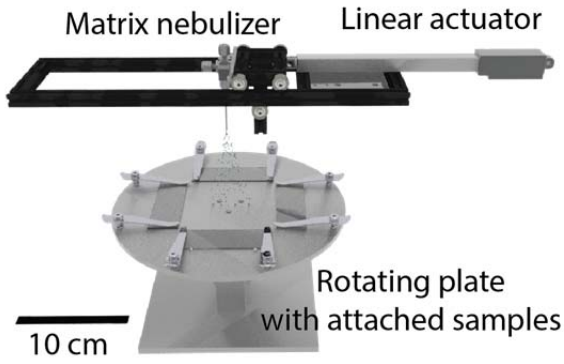

Figure S3. Three-dimensional depiction of the automated MALDI matrix coating system. Slides are affixed to the surface of a rotating disk with slide clamps. As the disk rotates (~ 7 Hz) the linear actuator oscillates the matrix nebulizer over the sample surface. As the center-to-nebulizer distance increases, the linear speed of the actuator decreases to compensate for the change in surface area covered by the spray.

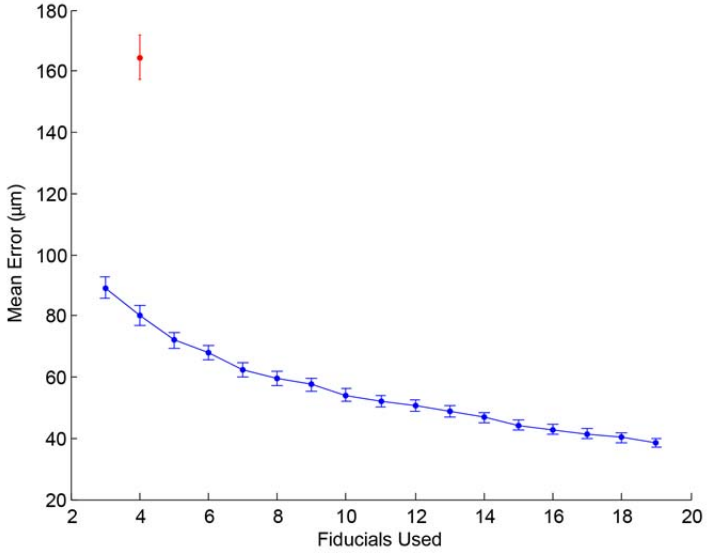

Figure S4. Comparison of the accuracy and robustness of geometric (red) and point-based (blue) registration transformation. To simulate uncertainty in fiducial location, Gaussian noise, $N(\mu = 0\ \mu m, \sigma = 100\ \mu m)$, was added to the x- and y-coordinates of the fiducial marks. Each point represents the mean ± SEM for 100 simulations of noise. As more fiducials are included in the model, the target localization error decreases below the added noise. To ensure accuracy, 10–15 fiducials were utilized for every slide.

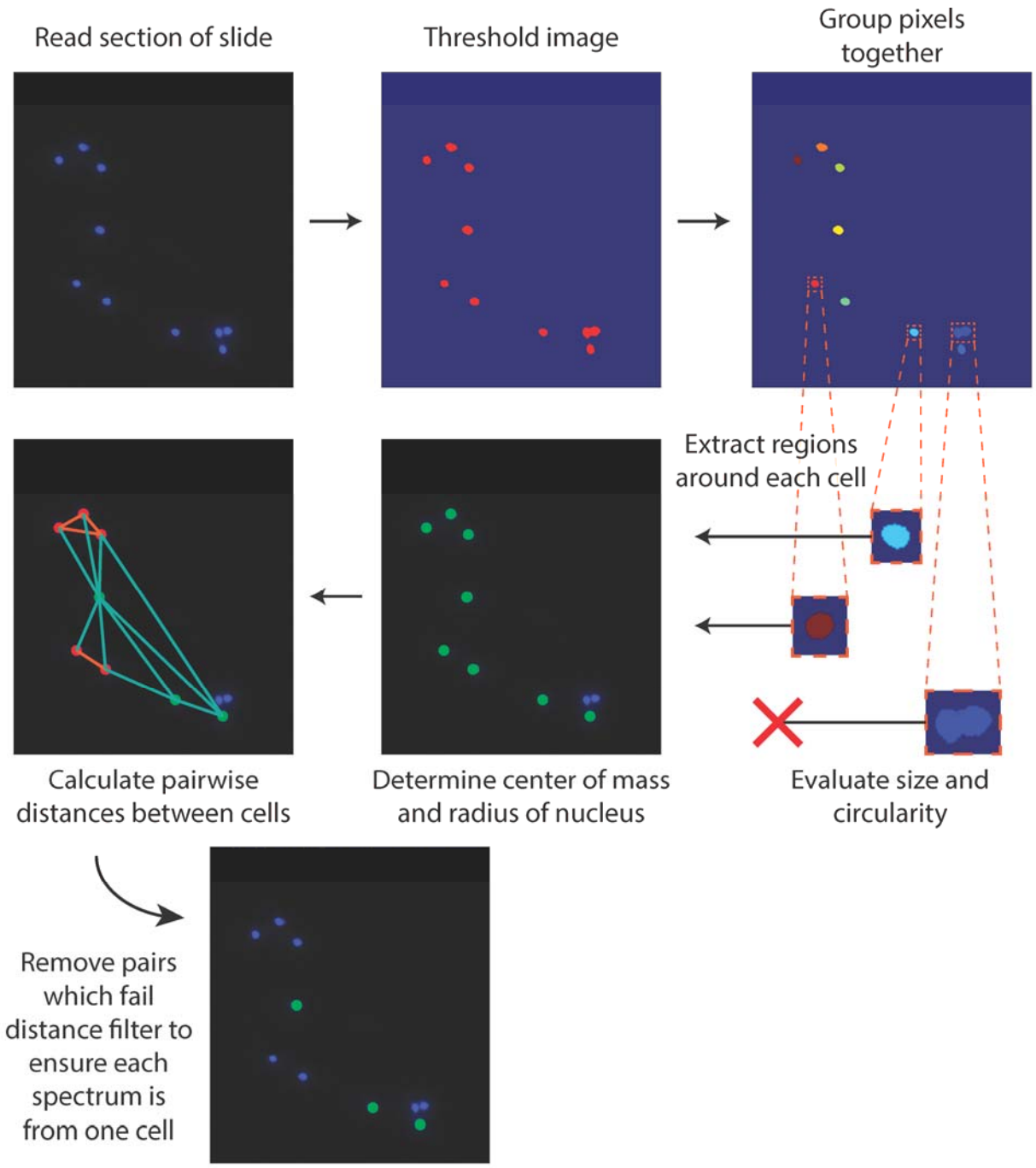

Figure S5. Overview schematic of the cell-finding algorithm. The high-contrast fluorescence images allow a simple threshold and group method to locate the center of each cell. Neighboring pixels are grouped together to generate a putative cell. Each possible cell is evaluated to determine if the intensity and circularity are within range, which eliminates background artifacts. Single cell locations are further evaluated by calculating the pairwise distance between each cell, eliminating those within 100 µm of each other.

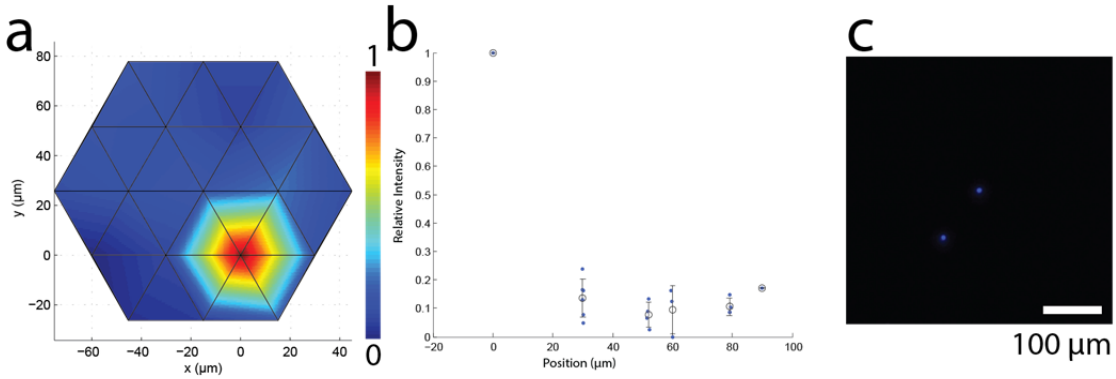

Figure S6. Insulin C-peptide redistribution from single cells after MALDI matrix application measured with MALDI MSI. (**a**) Representative figure of a hexagonally packed raster grid centered around single cells (point-to-point distance, 30 µm), analyzed for 18 β-cells on multiple ITO glass slides coated with matrix. (**b**) Defining the center point as the most intense position, the relative intensity as a function of distance from center showed a rapid drop in intensity after even a 30 µm step. Analysis of multiple spots indicated peptide spreading is limited to 50 µm from the center of the cell, where the intensity had dropped by ~90%. (**c**) All data utilized 100 µm as a cell-to-cell distance cut-off to exclude cells which were too closely located, and interfered with neighboring cells.

Table S1. Canonical and processed PP-peptides from islets of Langerhans detected with MALDI MS.

Peptide	PTM	Elemental composition*	Monoisotopic mass* (Da)	Observed mass (Da)	Mass error (ppm)
Insulin 1 (a+b chain)	3 internal disulfides	$C_{259}H_{388}N_{65}O_{75}S_6$	5800.687	5799.906	134.6
Insulin 2 (a+b chain)	3 internal disulfides	$C_{256}H_{383}N_{64}O_{76}S_7$	5793.612	5792.84	133.3
Glucagon		$C_{153}H_{226}N_{43}O_{49}S$	3481.624	3481.472	43.66
Somatostatin-14	1 internal disulfide	$C_{76}H_{105}N_{18}O_{19}S_2$	1637.724	1637.704	12.21
PP	C-terminal amidation	$C_{195}H_{299}N_{58}O_{57}S$	4397.2	4397.172	6.368
PP C-peptide	1 internal disulfide	$C_{128}H_{216}N_{37}O_{42}S_3$	3037.491	3037.415	25.02
PP(27-36)	C-terminal amidation	$C_{59}H_{95}N_{18}O_{15}$	1295.722	1295.71	9.261
PP(1-24)		$C_{124}H_{183}N_{32}O_{41}S$	2808.294	2808.231	22.43
PP(1-16)		$C_{81}H_{116}N_{19}O_{27}S$	1818.801	1818.76	22.54
PP(18-36)	C-terminal amidation	$C_{108}H_{174}N_{35}O_{30}$	2441.317	2441.257	24.58

*Masses are given as $[M+H]^+$